Effects of sub-cytotoxic exposure of silver nanoparticles on osteogenic differentiation of human bone marrow stem cells

Running Title: Osteogenic differentiation of hBMSC exposed to AgNP

Alexander K. Nguyen*,†, Reema Patel†, Roger Narayan*, Girish Kumar†, and Peter L. Goering†

*University of North Carolina/North Carolina State University Joint Department of Biomedical

Engineering, Raleigh, NC

[†]Office of Science and Engineering Laboratories, Center for Devices and Radiological Health, U.S. Food and Drug Administration, Silver Spring, MD

Keywords

- Silver nanoparticle
- Human bone marrow stem cell
- Osteogenic differentiation
- Hydroxyapatite
- Prolonged exposure

Abstract

Introduction: In vitro toxicology evaluations utilizing human stem cell models represent attractive alternatives to conventional animal models, which are not always predictive of human responses. Silver nanoparticles (AgNP) have been identified as a potent antimicrobial for use in orthopedic devices. However, AgNP exposure may alter the behavior of stem cells within the bone marrow. The aim of this study was to assess the effect of silver nanoparticles on osteogenic differentiation of human bone marrow mesenchymal stem cells (hBMSC).

Methods: PVP-coated 10nm AgNP were evaluated for their short-term (24 hr) cytotoxicity to hBMSC using the MTT assay to determine sub-cytotoxic concentrations for the subsequent long-term study investigating osteogenic differentiation. hBMSC were exposed to 0, 1, 5, or 10 μg/mL AgNP in three different exposure scenarios: Single (24 hr), Repeated (24 hr at 1, 7, 14 days), or Continuous (21 days) exposure in presence or absence of osteogenic supplements. Alkaline phosphatase (ALP) as an early osteogenic differentiation marker, hydroxyapatite deposition as a late marker, and cell proliferation were measured at days 1, 7, 14, and 21.

Results: AgNP exposure reduced cell proliferation compared to controls for all observed treatments. Neither ALP or hydroxyapatite expression was observed at any timepoint in hBMSC exposed to AgNP at 10 μg/mL in the presence of osteogenic supplements for any exposure scenario or for cells exposed to 5 μg/mL in the repeated or continuous exposure scenarios.

Conclusions: Long-term, *in vitro* AgNP exposure can influence hBMSC osteogenic differentiation and prevent substrate mineralization at AgNP concentrations not acutely cytotoxic.

Introduction

Infections associated with medical devices such as orthopedic implants are a common complication which often necessitates explantation of the device. Recently published statistics for total knee arthroplasty performed between 1999 and 2015 revealed infection in 1.0-1.5% of all orthopedic surgeries and was a close-second cause of revision surgeries. [1]. Staphylococcus was found to be the leading organism in orthopedic surgeries at 29%. [2]. This also includes methicillin resistant Staphylococcus aureus (MSRA), which does not respond well to antibiotic treatment. Due to the increasing risk of antibiotic-resistance, silver as an alternate mechanism for infection control would be advantageous. Incorporation of silver into medical devices is shown to reduce concentrations of various microbes including S. aureus and inhibit formation of biofilms [3, 4]. Both ionic and particulate forms of silver are used in skin-contacting medical devices such as wound dressings [5] or dermal reconstruction matrices [6], and multiple externalcommunicating devices such as Foley catheters containing silver are commercially available. Despite the beneficial anti-microbial properties, silver could have adverse effects to human cells if released in sufficient doses to the systemic circulation. For example, uncoated 35 nm AgNP were found to exceed the 5% hemolysis threshold in ASTM E2524-08 at 70µg/mL [7]. AgNP (12.5nm diam.) were also found to significantly alter several hematologic parameters at a 30µg/mL threshold concentration in a blood loop model [8].

Long-term silver exposure resulting from device implantation could raise the possibility of adverse local responses in the surrounding tissue. Stem cells in bone marrow play a role in a wide array of tissue regeneration tasks, such as growth of new bone, fat, and blood cells. While impairment of any of these functions might negatively influence patient treatment outcomes,

adverse effects on differentiation into the osteocyte lineage would slow or prevent osseointegration of the implant, leading to loosening, the leading cause of revision surgery. [1]

AgNP characteristics such as size, coating type, surface chemistry, etc. influence biological outcomes such as cytotoxicity, nanoparticle uptake, and intracellular localization [9] and the change of any one of these parameters can have drastic effects. For example, equimolar concentrations of 3, 10, 50, and 100 nm diameter AgNP had different effects on zebrafish mortality, and a number of sub-lethal effects such as malformation of different parts. [10] Thus, the large number of possible combinations would be a challenge to test with conventional animal models. An alternative in vitro model using human stems cells and allowing for long-term exposure to the toxicant of interest would not only be more relevant to human biological and toxicological responses, but also be more practical to evaluate a large number of potential toxicants. Therefore, the objective of this study was to assess the effect of prolonged AgNP exposure on osteogenic differentiation of human bone marrow mesenchymal stem cells (hBMSC) at sub-cytotoxic AgNP concentrations. Additionally, different exposure scenarios up to 21 days were investigated to model various degrees of duration (e.g., acute, moderate, prolonged) of implant tissue contact. Findings from this in vitro model can help inform further understanding of how human stem cells respond to sub-cytotoxic AgNP concentrations for extended exposures with additional benefits of 1) reducing the necessity of some animal testing, and 2) contributing to understanding risks and benefits of this material for medical device implant applications.

Methods and Materials

hBMSC (PCS-500-012, ATCC, Manassas, VA) were cultured in mesenchymal stem cell basal medium (PCS-500-030, ATCC, Manassas, VA) supplemented with the mesenchymal stem

cell growth kit (PCS-500-041, ATCC, Manassas, VA) and incubated at 37°C, 5.0% CO₂ and 90% relative humidity. Osteogenic differentiation was performed using the osteocyte differentiation tool (PCS-500-052, ATCC, Manassas, VA) in place of the medium. Other reagents included Trypsin-EDTA (9002-07-7, Sigma Aldrich, St. Louis, MO), Dulbecco's Phosphate Buffered Saline (14190-xxx, Thermo Scientific, Waltham, MA), Triton X-100 (Sigma Aldrich, St. Louis, MO), 37% formaldehyde (252549, Sigma Aldrich, St. Louis, MO), and ultrapure water from a NANOpure Diamond water purifier (APS Water Services Corp., Van Nuys, CA).

AgNP Characterization

PVP-coated, 10 nm diameter AgNP (BioPure, NanoComposix, San Diego, CA) were used in this study. AgNP stock solutions were received as a 1 mg/mL solution in water and were characterized using a JEM 2010F (JEOL, Tokyo, Japan) transmission electron microscope (TEM). Particles (n = 140) in one TEM image (Fig. 1) were analyzed using ImageJ (NIH, Bethesda, MD). Particle diameter averaged 9.95 nm with a standard deviation of 2.22 nm. The morphology was approximately circular with average major and minor elliptical axes of 10.52 and 9.44 nm, respectively. AgNP were dispersed in cell culture medium immediately before application to the cells per experimental design.

Cell Culture

For each experiment replicate, 1x10⁶ hBMSC stored in liquid nitrogen at passage 4 were thawed and seeded into a T-150 flask and incubated overnight. A media change was performed the following day to remove the DMSO cryopreservative and dead/unattached cells and then allowed to divide for approximately one week to reach 80% confluence. Cells were tryspinized,

centrifuged at 200 g for 5 min, and resuspended in media. The hBMSC suspension cell density was measured with a hemocytometer and diluted to 5.0 x 10⁴ cells/mL for seeding. Cells used in both the 24-hr exposure and 21-day culture procedures were therefore used at passage 5; passage 6 is the highest passage recommended by ATCC for osteogenic differentiation with the Osteocyte Differentiation Tool.

Viability of hBMSC after a single 24-hr exposure to AgNP

Cytotoxicity of AgNP in a single 24-hr exposure was measured via the MTT assay (CellTiter 96 Non-Radioactive Cell Proliferation Assay, G4000, Promega, Madison, WI) and read with an OptiMax plate reader (Molecular Devices, Sunnyvale, CA). Three wells per treatment in a 96-well plate were seeded with 1.0x10⁴ cells per well in 200 µL MSC media and allowed to attach over 24 hr. Cells were then exposed to 1, 5, 10, 25, or 50 µg/mL AgNP for 24 hr in either MSC basal medium or osteogenic medium. Medium alone and medium with 3 mM AgNO₃ were used as negative and positive controls, respectively. Cell-free wells of the corresponding solution were used as the background. An aliquot of 15 µL MTT dye was added to each well and allowed to metabolize for 3 hr. The kit surfactant solution was used to stop the reaction and dissolve the colored metabolite. The plates were read after 30 min incubation and 30 min on a shake plate. For each well, absorbance at 650 nm was subtracted from the absorbance at 570 nm. Viability is calculated as a percent of the negative control and reported as the means and standard deviations of three independent replicate experiments.

Long-term hBMSC culture using three dosing/exposure scenarios

Three long-term sub-cytotoxic exposure scenario studies involved monitoring hBMSC with a combination of the following treatment conditions: 1) exposure to one of three AgNP

dosing/exposure scenarios, 2) exposure to one of three different AgNP concentrations, and 3) culture in media with or without osteogenic supplements. The exposure scenarios are summarized in Figure 2: a single 24-hr exposure (Single), three 24-hr exposures performed on Days 1, 7, and 14 (Repeated), and a continuous exposure to AgNP for 21 days with AgNP refreshed 3X per week (Continuous). AgNP concentrations of 1, 5, or 10 µg/mL in media with (OS+) or without (OS-) osteogenic supplements were prepared immediately before exposure to the cells.

For each of four sampling timepoints (1, 7, 14, and 21 days), six 96-well plates were used corresponding to one of the three exposure conditions, and the use of media with or without osteogenic supplements. On each plate, two wells per AgNP concentration (1, 5 or 10 µg/mL) for each of the planned assays were seeded with $1.0x10^4$ cells per well in 200 µL medium and incubated for 24 hours before starting the prescribed exposure scenario. hBMSC grown with or without osteogenic supplements and in the absence of AgNP were used as the negative controls. Data from the negative controls are shared between all exposure scenarios but are included on all sub-charts in Figures 4, 5, 6, and 7 for ease of comparison. Media was changed three times a week for the 21-day culture period with either media or media with AgNP applied to the cells according to the relevant exposure scenario (Fig. 2). If a well in the Single or Repeated exposure scenarios received media with AgNP, the particles were removed 24 hr later and replaced with the corresponding media.

For each timepoint, plates were processed for the different assays: Quant-iT PicoGreen, ALP Liquicolor, and OsteoImage mineralization assays. ALP was measured immediately at each timepoint but PicoGreen and OsteoImage assays were performed in bulk after all plates had been harvested. In preparation for storage, media were aspirated from all wells; OsteoImage wells

were fixed with 3.7% formaldehyde in PBS for 30 min, rinsed 2X with PBS, then the PBS aspirated before storage at -80°C.

PicoGreen assay

Cells designated for the PicoGreen assay (Quant-iT PicoGreen dsDNA assay kit, P7589, Thermo Scientific, Waltham, MA) were previously frozen at -80°C so were thawed to room temperature before digestion with a papain suspension (lot 32J13550, LS003127, Worthington, Lakewood, NJ). Papain was dissolved at a 0.21 U/mL concentration in 1.75 mg/mL L-cysteine in PBS, and 200 µL of this solution was added to each well. The entire plate was sealed with aluminum sealing tape and heated at 60°C for 18 hr. After digestion, the plates were cooled for 1 hr. From each well, three aliquots of 50 µL was transferred to three wells on a separate 96-well plate for measurement in triplicate. A double-stranded DNA concentration series (0, 40, 100, 200, 400, 600, 1000, 1400, 1600, and 2000 ng/mL) was prepared by diluting the kit dsDNA stock solution in Tris-EDTA buffer. For each dsDNA ladder concentration, 50 µL was added to two wells for measurement in duplicate. PicoGreen dye in Tris-EDTA buffer was mixed according to the manufacturer's specifications and 50 µL was added to all wells and the samples stained for 5-10 min. The plate was read in a fluorescent plate reader using 485 nm excitation and 538 nm emission wavelengths. For each set of three measurement wells corresponding to a single well on the initial plate, the average fluorescence intensity was fit to the DNA standard curve and multiplied by the 200-µL volume used in the papain digestion to calculate the DNA mass within the well.

Alkaline phosphatase (ALP) assay

ALP was measured using the Alkaline Phosphatase Liquicolor kit (2900-430, Stanbio, Boerne, TX) using SER-T-FY 1 Level 1 Control Serum (lot 151631, G427-86, Stanbio, Boerne, TX) for controls. Kinetic measurements for this assay were performed on a SpectraMax 190 plate reader (Molecular Devices, Sunnyvale, CA). Media from ALP assay wells were aspirated and replaced with 100 µL 0.2% Triton X-100 in PBS for 20 min. A new 96-well plate was prepared where three wells each were allocated for negative and positive controls: 0.2% Triton X-100, 5 μL serum, 15 μL serum, and 35 μL serum. These control wells were diluted to 75 μL total volume with additional 0.2% Triton X-100. The permeabilized cells were diluted with an additional 100 µL of 0.2% Triton X-100 and mixed thoroughly. Two 75 µL aliquots from each of these solutions were added to two wells on the new plate for measurement in duplicate. A 75 μL aliquot of the kit working reagent was added to each well, then the plate was immediately placed into a fluorescent plate reader for kinetic measurements. Absorbance at 405 nm was read once per min over 5 hr. The rate of generation of the colored compound is initially linear and proportional to the ALP content. For each well, the linear region of the curve was determined between the start of data collection and the timepoint when the R² value of the linear regression was greater than 0.98. The slope of the linear region was compared to the slope of the serum control wells to calculate the ALP concentration.

OsteoImage fluorescent microscopy/mineralization quantification assay

Mineralization quantification was performed with the OsteoImage Mineralization assay (PA-1503, Lonza, Walkersville, MD) that specifically stains hydroxyapatite; fluorescence quantification using a plate reader and fluorescence microscopy were performed in the same well. The hBMSCs were previously fixed in 3.7% formaldehyde and stored frozen at -80°C. OsteoImage dye was diluted 1:100 in the supplied wash buffer per manufacturer's instructions;

100 μL was added to each well, the samples stained for 30 min, then washed 3X with the wash buffer. Hydroxyapatite fluorescence signal was read at 492 nm excitation and 520 nm emission wavelengths. Fluorescent images of the wells after 21 days in culture were obtained using an Eclipse TE2000-U fluorescence microscope (Nikon, Tokyo, Japan).

Statistical analysis

Statistical analysis and graphing were performed using Graphpad Prism 6 (San Diego, CA). Cytotoxicity after 24-hr AgNP exposure was analyzed by multiple Student's t-test comparing each treatment to the negative control. Proliferation during the 21-day study measured by the Pico Green DNA assay was analyzed using two-way ANOVA between AgNP concentrations and exposure scenarios within each timepoint; statistical significance was determined using the Tukey *post hoc* analysis (p < 0.05). Detection of ALP and mineralization, early and late markers of osteogenic differentiation respectively, was analyzed by comparing OS+ supplemented cells to the corresponding OS- treatment for each timepoint using a one-tailed Students t-test. Since both ALP expression and hydroxyapatite deposition were near baseline levels for all OS- cells, data was summarized as the difference between the OS+ and OS- supplemented groups for clarity. Thus, the resulting means and standard deviations were calculated using $\bar{X}_{OS+} - \bar{X}_{OS-} \pm \sqrt{SD_{OS+}^2 + SD_{OS-}^2}$.

Results

Dose finding for cytotoxicity of AgNP after a single 24-hr exposure

An AgNP concentration-dependent decrease in hBMSC viability was observed using the MTT assay (Fig. 3). Based on the international standard ISO 10993-5 [11], a chemical is noted to

have cytotoxic potential if the viability falls below 70%. Viability of hBMSC exposed to 1 or 5 μg/mL AgNP for 24 hr was not statistically different from the negative control. hBMSC exposed to 10 μg/mL AgNP exhibited viabilities of 80% and 71% of control when cultured in the absence and presence of osteogenic supplements, respectively. Concentrations of 25 and 50 μg/mL resulted in statistically significant decreases in viability and the values were below the 70% cytotoxicity threshold. Therefore, concentrations of 1, 5, and 10 μg/mL AgNP concentrations were utilized for the subsequent long-term exposure studies.

Cell proliferation

Proliferation was assessed with the PicoGreen assay in which dsDNA concentrations can be quantitatively measured. The dsDNA concentration is proportional to the number of live cells remaining in culture; dead cells detach from the plate and are removed with regular media changes. For easier data visualization, proliferation data was organized in two graphs; as a time course (Fig. 4) and individually by timepoint to more clearly show the dose response and statistically significant differences (Fig. 5).

Behavior of undifferentiated and differentiating hBMSC is observed when considering the proliferation data as a time course (Fig. 4). Long-term cell culture of hBMSC without osteogenic supplements (OS-) was supported over the 21-day study with increasing proliferation observed at all timepoints under control conditions, which is as expected for a stem cell population. This increasing proliferation was also observed after Single exposure to 1 μg/mL AgNP. No change in proliferation was observed after Single exposure to 10 μg/mL, Single or Repeated exposure to 5 μg/mL, or with Repeated exposure to 1 μg/mL AgNP. In contrast, hBMSC exposed to osteogenic supplements (OS+) under control conditions proliferated between Day 1 and 7 after which the amount of dsDNA decreased at Day 14 and 21. In general,

differentiated cells do not proliferate so the decrease in dsDNA mass was expected for a differentiated culture. Cell proliferation under all exposure conditions of 1 or 5 μ g/mL AgNP responded similarly as the control with high proliferation apparent at Day 7. Proliferation under Continuous exposure to 1 μ g/mL AgNP also shows some proliferation at Day 7; however, no increase in proliferation is observed at Single or Repeated exposure at 10 μ g/mL or Continuous exposure at 5 or 10 μ g/mL.

At Day 1, no statistically significant difference in dsDNA content was found between any AgNP concentration or exposure scenario (Fig. 5). By Day 7, evidence of a dose-related response was becoming evident, with proliferation in the 1 μg/mL AgNP treatment group significantly higher than in the 10 μg/mL group for both the OS+ supplemented and OS- cells. This dose response was also observed at Day 14 and 21 within each exposure scenario. Proliferation resulting from Continuous exposure tended to be lower at all AgNP concentrations than the Single or Repeated exposure scenarios, although the differences between exposure scenarios using the same AgNP concentration were not statistically significant.

Assessment of early and late osteogenic differentiation markers

ALP expression as an early marker of osteogenic differentiation and hydroxyapatite content as a late marker of differentiation is displayed in Figure 6 and Figure 7 respectively. As with the proliferation data, only one set per replicate of 0 µg/mL AgNP exposure was performed but is included on all charts for convenience. In both assays, intensity of the signal should only be used to detect whether osteogenic differentiation was taking place at a certain timepoint. This is due to the coarse nature of the timepoints preventing precise measurement of when the signal is first observed. For example, ALP expression should increase until around day 14 and decrease afterwards but the exact time of the peak is unknown; comparison of one treatment group at the

ALP expression peak and a second that had expressed it slightly earlier and has a smaller signal would yield false conclusions. Therefore, the ALP or hydroxyapatite signal for the OS+ supplemented cells were only compared to the corresponding OS- group for statistical analysis. ALP and hydroxyapatite signal were also near baseline for all cells not exposed to osteogenic supplements, so the data were displayed as the difference between the two groups for clarity.

In hBMSC cultured in the presence of osteogenic supplements under control conditions, ALP expression reached a peak after 14 days in culture with detectable increases by day 7 (Fig. 6). hBMSC exposed to 1 μg/mL in all exposure scenarios or exposed to a Single exposure to 5 μg/mL had significantly increased ALP levels at day 7 and expressed detectable levels of hydroxyapatite at day 21 (Fig. 7). Of these, all treatment groups except for Single exposure to 5 μg/mL AgNP and Repeated exposure to 1 μg/mL had detectable hydroxyapatite at day 14; the corresponding fluorescence images of mineralized substrates after 21 days in culture is displayed in Figure 8. Thus, detection of ALP at day 7 is highly predictive of eventual mineralization of the substrate.

Discussion

The broad anti-microbial properties of AgNP makes them attractive for use in medical device materials; however, these benefits must be balanced with the potential effects on surrounding tissue. Traditional cytotoxicity testing as described in the ISO 10993 Part 5 standard [11] specifies that a 70% viability after 24 hr exposure is considered as "cytotoxic potential". The mechanism of AgNP cytotoxicity is an active area of research with particle parameters such as diameter, surface charge, geometry, and ion dissolution playing a role.[9, 12] Thus, one would expect different degrees of cytotoxicity responses when considering particles of different diameters and/or coatings. For example, Sengstock et al. reported no observable

change in hBMSC viability in 50 nm, PVP-coated AgNP over 24 hr exposure to 10 μg/mL AgNP [13], whereas the current study demonstrated a decrease in viability of hBMSC to the 70% viability threshold when 10 nm PVP-coated AgNP were used, which suggests that smaller diameter nanoparticles are more cytotoxic. Rosario et al. reports a viability reduction to 90% of control for MG-63 human osteosarcoma cells exposed to 10 μg/mL 10 nm PVP-coated AgNP exposure and reaches the 70% viability threshold at 50 μg/mL. [14] The current study using primary stem cells exposed to 10 nm PVP-coated AgNP from the same supplier resulted in the 70% viability threshold at 10 μg/mL. Similarly, a 24-hr exposure of immortalized human skin keratinocyte cells [15] and MCF-7 breast cancer cells [16] to 10 μg/mL of uncoated 20 nm AgNP resulted in cell viabilities of 67% and 76%, respectively. Exposure of various cell types to 24 hr to 10 μg/mL of both PVP and uncoated AgNP were found to have no observed cytotoxic effect or meet the threshold as a potential cytotoxicant. These results support the findings in the current study that identify 1 and 5 μg/mL 10 nm PVP-coated AgNP concentrations as subcytotoxic and 10 μg/mL as a concentration with borderline cytotoxic potential.

Prolonged or permanent exposure to a medical device implant requires further evaluation beyond 24-hr cytotoxicity testing and includes, but is not limited to, longer-term animals tests for systemic toxicity, skin sensitization and irritation, and implantation. In this study, in vitro exposure of hBMSC to AgNP up to 21 days revealed significant differences in proliferation and markers of osteogenic differentiation. Castiglioni et al. reported a dose-dependent cytotoxicity to 35 nm uncoated AgNP with a decrease in Saos-2 osteoblast-like cell viability to approximately 90% of control after a 5-day exposure to 1 and 5 μg/mL and a similar decrease to approximately 70% for 10 μg/mL exposures [17]. In addition, these AgNP were not found to affect differentiation of hBMSC into osteoblasts after 15 days in culture as judged by

Alizarin Red staining of calcium deposits. Nanoparticle size plays a significant role in many in vitro endpoints except for DNA damage; exposed particle surface area was identified as a major factor influencing biological responses [9] and could explain some of the discrepancy between these studies. Since 10 nm AgNP has 3.5 times the surface area of 35 nm AgNP per unit mass, the surface area of 5 µg/mL concentration of 10 nm AgNP would therefore roughly corresponds to the surface area in 17.5 μ g/mL of 35 nm AgNP; this is within the range of 10 – 25 μ g/mL 35 nm AgNP used by Castiglioni showing calcium deposition after 15 days. Continuous exposure to 5 μg/mL AgNP in this study resulted in cytotoxicity at the 7-day timepoint and no evidence of osteogenic differentiation was observed; thus, factors in addition to surface area appears to play a role in predicting toxicity. One possible explanation is that particle size affects uptake and intracellular localization that can have location-dependent toxic effects. Uptake studies in human fibroblasts revealed that 30 nm gold nanoparticles are retained within the cytoplasm while 5 nm gold nanoparticles were found within the nucleus [18]. Particle uptake studies in human mesenchymal stem cells exposed to 70 nm AgNP demonstrated perinuclear localization [19]. Uncoated[20] and PVP-coated[21] 10 nm AgNP were also localized within lysosomes in multiple cell lines. Nano-scale ionic silver crystals were also found and attributed to the dissolution of ionic silver from AgNP due to the acidic environment within lysosomes; silver ions could precipitate due to presence of intracellular chloride and thiol-containing compounds.[21]

Dissolution of silver ions from AgNP plays a major role in AgNP toxicity. Rosario et. al reported a greater cytotoxic response in MG-63 cells from AgNO₃ compared to the corresponding mass of AgNP for exposures up to 48 hr but noted that by 7 days of exposure to 5 µg/mL 10 nm AgNP, MG-63 cells lost all proliferative capacity determined by the clonogenic

assay while the corresponding 5 μg/mL of Ag⁺ ions had significantly reduced proliferative capacity [14]. In the present study, it is possible that cytotoxicity observed in the Continuous exposure scenario could have been due to a larger contribution from intracellular particles compared to the Single or Repeated exposures. This conjecture is supported by the proliferation of hBMSC in the Single and Repeated exposures at 1 μg/mL being statistically different from the proliferation in the Continuous exposure at day 14 for hBMSC cultured with osteogenic supplements. The trend appears to continue for day 21 although the difference between 1 μg/mL Repeated and Continuous exposures was not statistically significant.

Other studies support that the effect on AgNP on hBMSC proliferation could be partially attributed to early molecular initiating events, such as the dysregulation of genes related to cell metabolism or reactive oxygen species (ROS) defense, that lead to cytotoxicity. Genes related to osteogenesis were upregulated after 24-hr exposure to 20 µg/mL of 20nm AgNP to the MC3T3-E1 mouse osteoblast cell line [22]. Similarly, a decrease in proliferation in hBMSC and upregulation of markers related to endoplasmic reticulum and ROS stresses were found but no change to osteogenic differentiation markers were found in hBMSC [23]. Calcium deposition can be considered a definitive marker of successful osteogenic differentiation; hBMSC exposure to 10 and 25 µg/mL 35nm AgNP over 5 days in another study did not cause a change in calcium deposition [17]. In contrast, ALP and mineralization in the current study were significantly impaired for most of the investigated concentrations and exposure scenarios. These effects occurred concomitantly with a marked decrease in proliferation, which may represent a cytotoxic response rather than impairment of differentiation.

Conclusion

The present study examines the effect of different exposure scenarios on the proliferation and osteocyte function of differentiated hBMSC. Notably, a cytotoxic threshold of 10 µg/mL PVP-coated 10nm AgNP for hBMSC was determined but this single 24-hr exposure caused a loss of osteocyte function in the 21-day culture. Viability of hBMSC exposed to 5 µg/mL was not significantly different from controls in the 24-hr exposure but this Single 24-hr exposure caused a delay in the observation of ALP. This marker and subsequent mineralization was not observed after Repeated 24-hr exposures at the 5 µg/mL concentration. hBMSC exposed to the 1 µg/mL AgNP concentration were observed to express ALP and deposit hydroxyapatite in all exposure scenarios but Continuous exposure caused significantly lower proliferation rates than the other two exposure scenarios at day 14.

The well-known ability of silver to prevent growth of a broad spectrum of infectious organisms without the use of antibiotics makes it an attractive additive to medical device implants. However, AgNP exposure at sufficient concentrations and/or exposure durations does have an adverse effect on hBMSC osteogenic differentiation and subsequent function as osteocytes. AgNP-containing medical device materials must be carefully formulated and evaluated to determine the benefit of infection control versus the risk of adverse effects to bone marrow. [24]

Evaluating nanomaterials with biomedical applications presents challenges due to the vast number of nanoparticle physical and chemical parameters (e.g., size, shape, and coating) that influence biological and toxicological effects. For example, assumptions about the safety and performance of AgNP might not be supportable if there is a change in one or more of these parameters. Due to the vast number of nanomaterials with varying sizes, shapes, surface coatings and chemistries, and routes of exposure, *in vitro* human stem cell models that offer

prolonged exposure scenarios compared to traditional in vitro models, represent a potentially valuable component of integrated test strategies to evaluate nanomaterials.

Acknowledgments

The study was supported by funds from the USFDA.

Disclosure Statement

The authors have no conflicts of interest.

Disclaimer

The findings and conclusions in this paper have not been formally disseminated by the Food and

Drug Administration and should not be construed to represent any agency determination or

policy. The mention of commercial products, their sources, or their use in connection with

material reported herein is not to be construed as either an actual or implied endorsement of such

products by Department of Health and Human Services.

Correspondence Address

Peter L. Goering, PhD, DABT, ATS

Division of Biology, Chemistry, and Materials Science

Office of Science and Engineering Laboratories

Center for Devices and Radiological Health

US Food and Drug Administration

10903 New Hampshire Ave

Silver Spring, MD 20993

Email: Peter.Goering@fda.hhs.gov

19

References

- Chua, H.S., S.L. Whitehouse, M. Lorimer, et al., Mortality and Implant Survival With Simultaneous and Staged Bilateral Total Knee Arthroplasty Experience From the Australian Orthopaedic Association National Joint Replacement Registry. J Arthroplasty, 2018.
- 2. Al-Mulhim, F.A., M.A. Baragbah, M. Sadat-Ali, et al., Prevalence of surgical site infection in orthopedic surgery: a 5-year analysis. Int Surg, 2014. **99**(3): p. 264-8.
- 3. Goel, A., M.K. Meher, P. Gupta, et al., Microwave assisted κ-carrageenan capped silver nanocomposites for eradication of bacterial biofilms. Carbohyd Polym, 2019. **206**: p. 854-862.
- Khalid, H.F., B. Tehseen, Y. Sarwar, et al., Biosurfactant coated silver and iron oxide nanoparticles with enhanced anti-biofilm and anti-adhesive properties. J Hazard Mater, 2019.
 364: p. 441-448.
- 5. Liu, M., T. Liu, X. Chen, et al., Nano-silver-incorporated biomimetic polydopamine coating on a thermoplastic polyurethane porous nanocomposite as an efficient antibacterial wound dressing.

 J Nanobiotechnol, 2018. **16**(1): p. 89.
- 6. Chen, Y., N. Dan, W. Dan, et al., A novel antibacterial acellular porcine dermal matrix cross-linked with oxidized chitosan oligosaccharide and modified by in situ synthesis of silver nanoparticles for wound healing applications. Mater Sci Eng C Mater Biol Appl, 2019. **94**: p. 1020-1036.
- 7. Choi, J., V. Reipa, V.M. Hitchins, et al., Physicochemical Characterization and In Vitro Hemolysis Evaluation of Silver Nanoparticles. Toxicol Sci, 2011. **123**(1): p. 133-143.
- 8. Krajewski, S., R. Prucek, A. Panacek, et al., Hemocompatibility evaluation of different silver nanoparticle concentrations employing a modified Chandler-loop in vitro assay on human blood.

 Acta Biomaterialia, 2013. **9**(7): p. 7460-7468.

- Ahmed, K.B.R., A.M. Nagy, R.P. Brown, et al., Silver nanoparticles: Significance of physicochemical properties and assay interference on the interpretation of in vitro cytotoxicity studies. Toxicol In Vitro, 2017. 38: p. 179-192.
- 10. Bar-Ilan, O., R.M. Albrecht, V.E. Fako, et al., Toxicity assessments of multisized gold and silver nanoparticles in zebrafish embryos. Small, 2009. **5**(16): p. 1897-910.
- International Organization for Standardization. Biological Evaluation of medical devices. (ISO Standard No. 10993:2009). Retrieved from https://www.iso.org/standard/36406.html
- 12. De Matteis, V., M. Cascione, C.C. Toma, et al., Silver Nanoparticles: Synthetic Routes, In Vitro Toxicity and Theranostic Applications for Cancer Disease. Nanomaterials (Basel), 2018. **8**(5).
- 13. Sengstock, C., J. Diendorf, M. Epple, et al., Effect of silver nanoparticles on human mesenchymal stem cell differentiation. Beilstein J Nanotechnol, 2014. **5**: p. 2058-2069.
- 14. Rosario, F., P. Hoet, C. Santos, et al., Death and cell cycle progression are differently conditioned by the AgNP size in osteoblast-like cells. Toxicology, 2016. **368-369**: p. 103-115.
- 15. Kreeinthong, S. and P. Uawithya, Effects of Short-Term Silver Nanoparticle Exposure on Proliferative Signaling Pathway in Human Skin Keratinocyte. J Physiol Biomed Sci., 2014. **27**(2): p. 48-53.
- 16. ÇİFtÇİ, H., M. TÜRk, U. Tamer, et al., Silver nanoparticles: cytotoxic, apoptotic, and necrotic effects on MCF-7 cells. Turkish J Biol, 2013. **37**(5): p. 573-581.
- 17. Castiglioni, S., A. Cazzaniga, L. Locatelli, et al., Silver Nanoparticles in Orthopedic Applications:

 New Insights on Their Effects on Osteogenic Cells. Nanomaterials, 2017. **7**(6).
- 18. Berry, C.C., J.M. de la Fuente, M. Mullin, et al., Nuclear localization of HIV-1 tat functionalized gold nanoparticles. IEEE Trans Nanobioscience, 2007. **6**(4): p. 262-9.

- 19. Ahlberg, S., A. Antonopulos, J. Diendorf, et al., PVP-coated, negatively charged silver nanoparticles: A multi-center study of their physicochemical characteristics, cell culture and in vivo experiments. Beilstein J Nanotechnol, 2014. **5**(5): p. 1944-1965.
- 20. Hsiao, I.-L., Y.-K. Hsieh, C.-Y. Chuang, et al., Effects of silver nanoparticles on the interactions of neuron- and glia-like cells: Toxicity, uptake mechanisms, and lysosomal tracking. Environ Toxicol, 2017. **32**(6): p. 1742-1753.
- 21. Wildt, B.E., A. Celedon, E.I. Maurer, et al., Intracellular accumulation and dissolution of silver nanoparticles in L-929 fibroblast cells using live cell time-lapse microscopy. Nanotoxicology, 2016. **10**(6): p. 710-9.
- 22. Qing, T., M. Mahmood, Y. Zheng, et al., A genomic characterization of the influence of silver nanoparticles on bone differentiation in MC3T3-E1 cells. J Appl Toxicol, 2018. **38**(2): p. 172-179.
- 23. Pauksch, L., S. Hartmann, M. Rohnke, et al., Biocompatibility of silver nanoparticles and silver ions in primary human mesenchymal stem cells and osteoblasts. Acta Biomater, 2014. **10**(1): p. 439-49.
- 24. Petrochenko, P.E., J. Zheng, B.J. Casey, et al., Nanosilver-PMMA composite coating optimized to provide robust antibacterial efficacy while minimizing human bone marrow stromal cell toxicity.

 Toxicol In Vitro, 2017. **44**: p. 248-255.

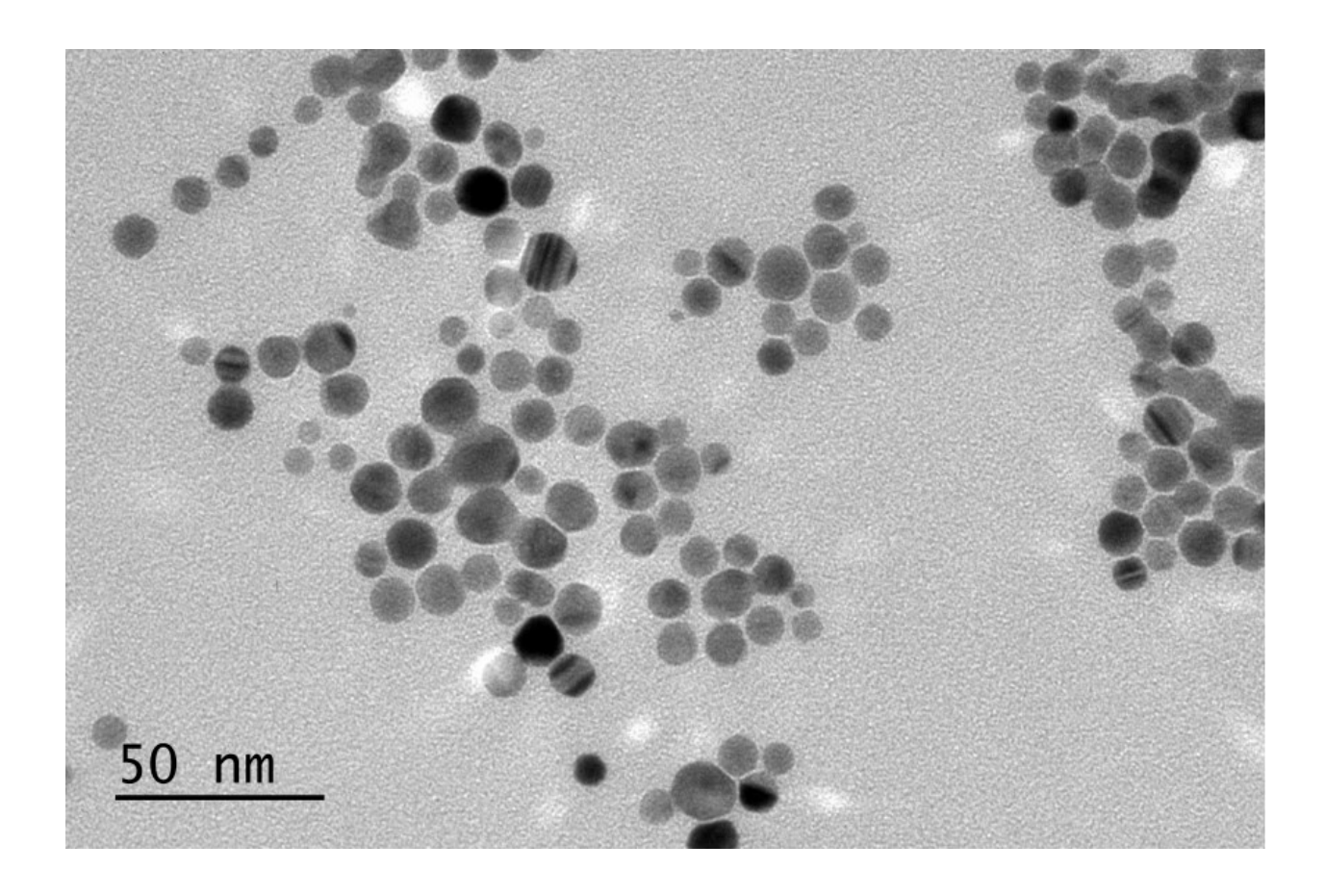


Figure 1 - TEM image of 10nm PVP-coated AgNP. AgNP core diameter was determined to be 9.95 nm with a 2.22 nm standard deviation by image analysis of n=140 particles.

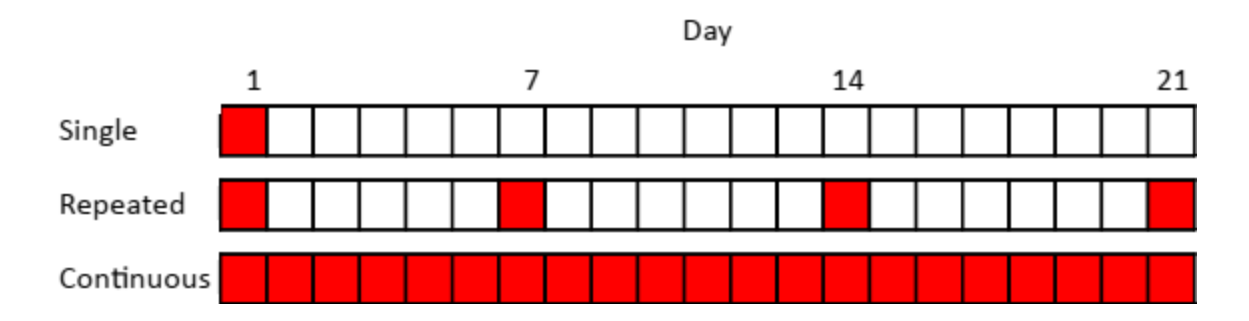


Figure 2 - Schedule of AgNP dosing of hBMSC cultures for three separate exposure scenarios: Single 24-hr exposure, Repeated weekly 24-hr exposures, or Continuous exposure. Each square represents a 24-hr period with red squares indicating periods of AgNP exposure. Cell proliferation, alkaline phosphatase expression, and hydroxyapatite content were measured on Days 1, 7, 14, and 21 for all exposure scenarios. Fluorescence imaging of hydroxyapatite was performed on Day 21 only.

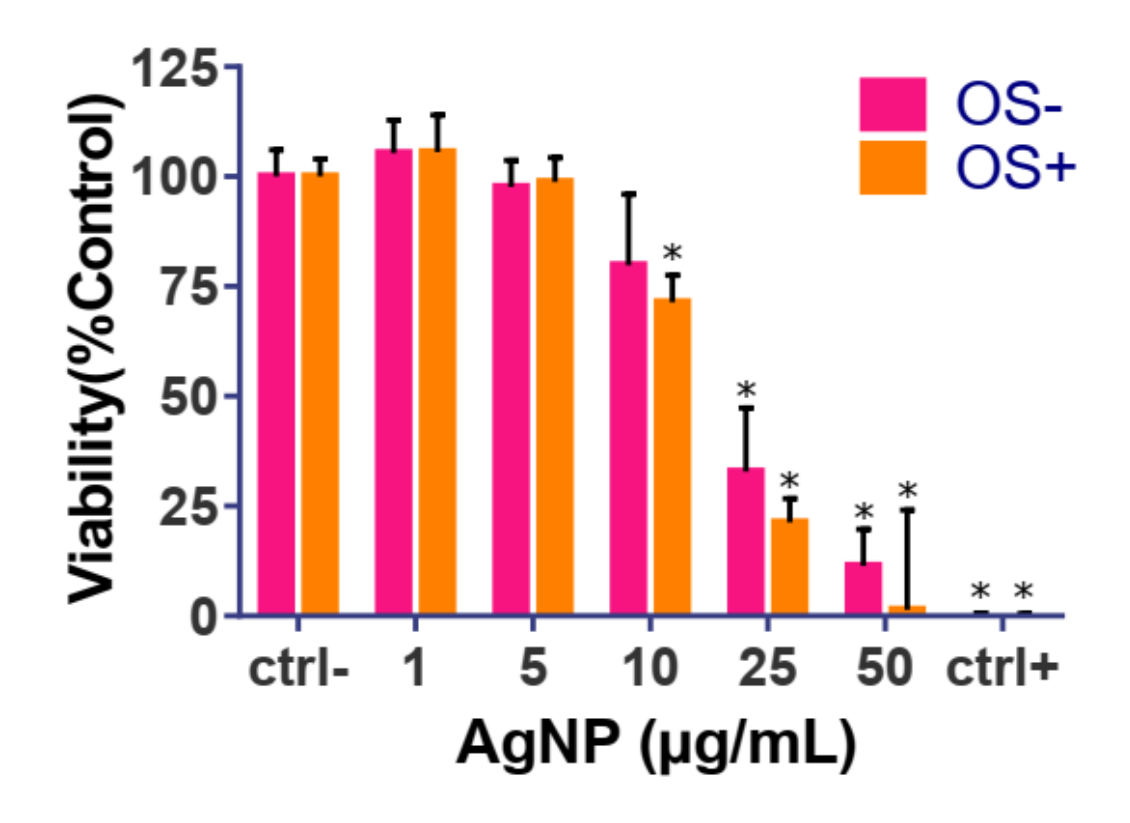


Figure 3 – Viability of hBMSC (MTT assay) cultured for 24 hr in the absence (OS-) or presence (OS+) of osteogenic supplements. Cells were exposed to various concentrations 10 nm PVP-coated AgNP. Cells grown in media alone or media with 3 mmol/L AgNO₃ were used as the negative (ctrl-) and positive (ctrl+) controls, respectively. Values represent $\bar{x} \pm SD$ (n = 3 replicate experiments). Bars with asterisks are significantly different than the negative control (p < 0.05)

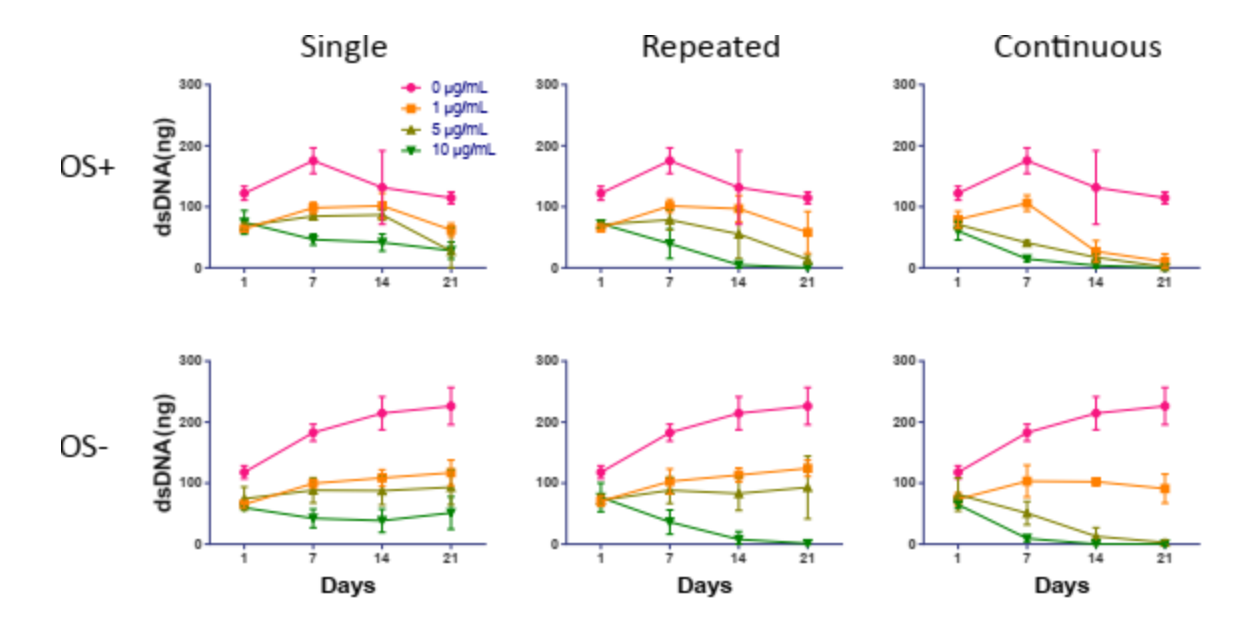


Figure 4 – Time course responses for proliferation of hBMSC (PicoGreen dsDNA assay) cultured in the absence (OS-) or presence (OS+) of osteogenic supplements under Single, Repeated, or Continuous exposure (see Fig. 2) to 1, 5, or 10 μ g/mL of 10 nm PVP-coated AgNP. Note that hBMSC not exposed to OS (OS-) or AgNP proliferated over the entire 21-day period while proliferation of hBMSC exposed to OS (OS+) peaked around Day 7 and then declined. Values represent $\bar{x} \pm SD$ (n = 3 replicate experiments). Statistical analysis of these data is displayed in Figure 5.

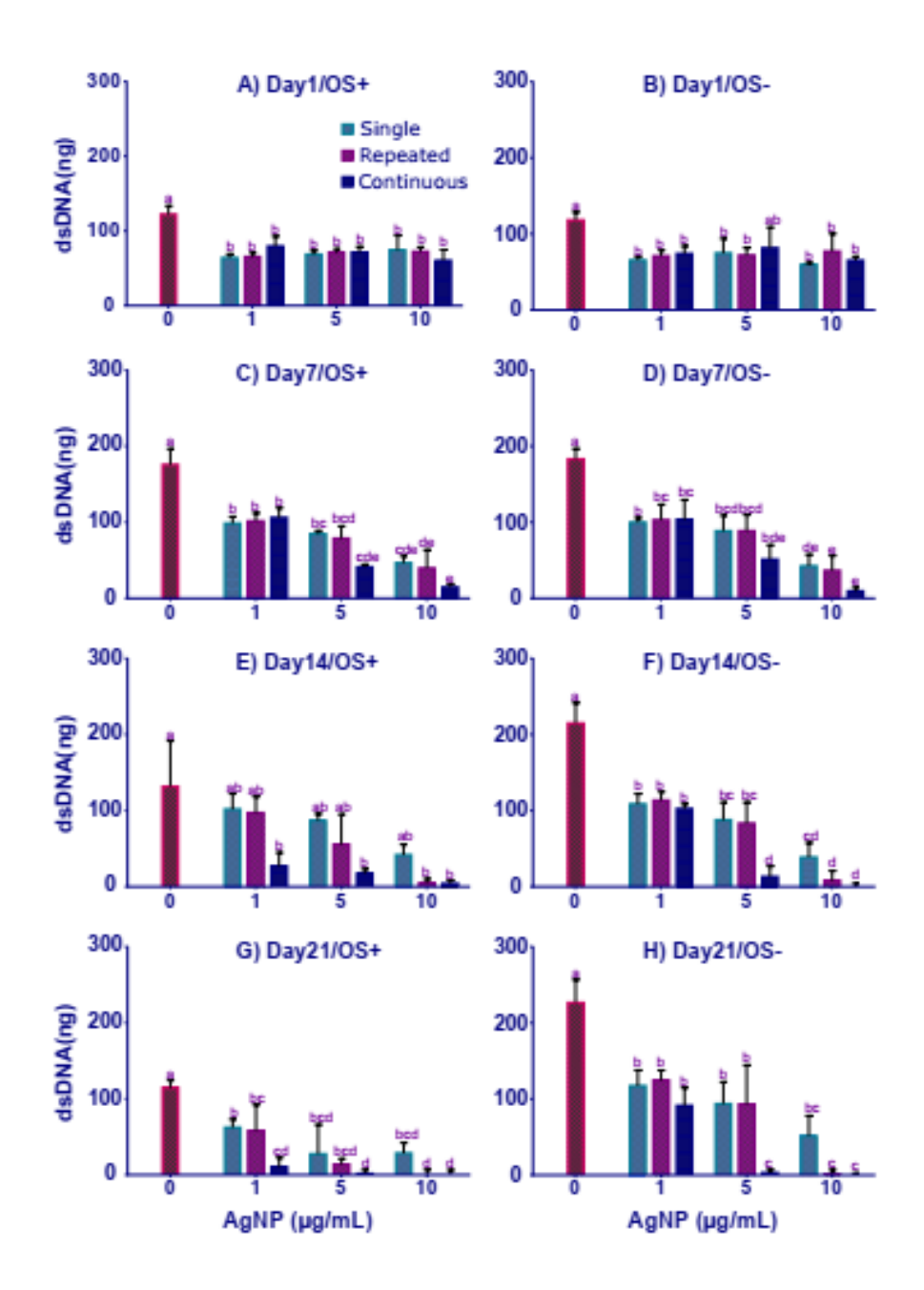


Figure 5 – Cell proliferation data from Fig. 4 plotted separately for Days 1, 7, 14, and 21 of culture to more clearly show statistical differences of exposure (Single, Repeated, Continuous) scenario and AgNP dose. Values represent $\bar{x} \pm SD$ (n=3). Bars with no matching letters are statistically different (p < 0.05).

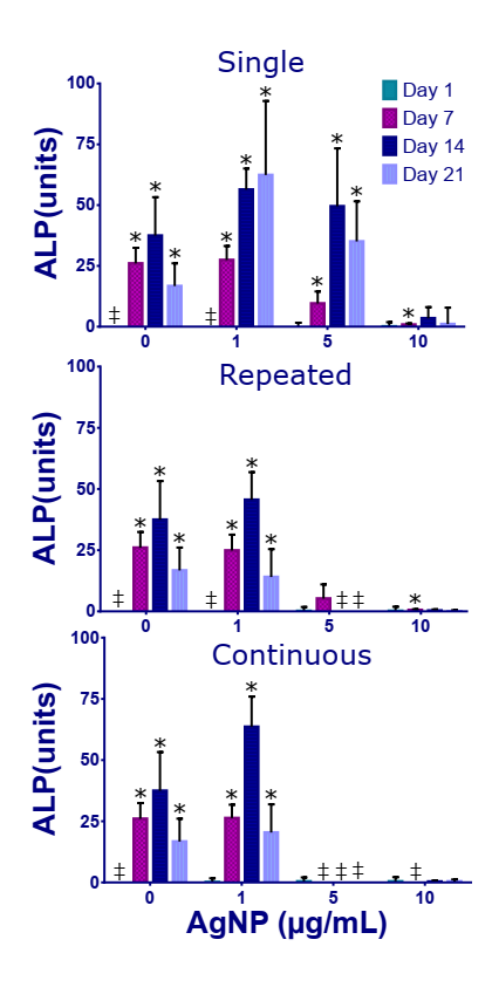


Figure 6 – Differences in alkaline phosphatase (ALP) expression in hBMSC cultured in the presence (OS+) and absence of (OS-) of osteogenic supplements under Single, Repeated, or Continuous exposure (see Fig. 2) to 1, 5, or 10 μg/mL of 10 nm PVP-coated AgNP. Elevated ALP expression is an early marker of osteogenic differentiation. Values plotted were derived by subtracting the signal values from OS- cells from the signals from OS+ supplemented cells.

Therefore, the values represent $\bar{x} \pm SD$ calculated as $\bar{X}_{OS+} - \bar{X}_{OS-} \pm \sqrt{SD_{OS+}^2 + SD_{OS-}^2}$ for n = 3 replicate experiments. Bars with asterisks denote a statistically significant (p < 0.05) increase in ALP expression of OS+ supplemented cells over the corresponding OS- cells. Absent bars marked with ‡ are the result of negative values due to subtracting the signal values from OS- cells from near-baseline signals from OS+ supplemented cells.

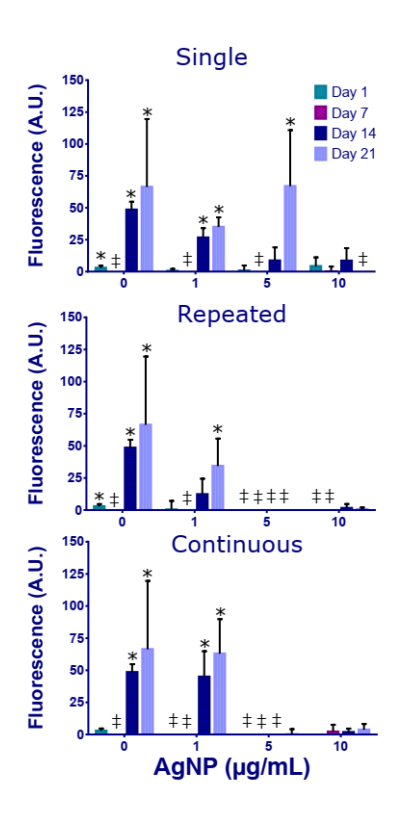


Figure 7 – Differences in hydroxyapatite content (Osteoimage Mineralization assay) between tissue culture polystyrene surfaces (TCPS) with hBMSC cultured in the presence of osteogenic supplements (OS+) subtracted from TCPS with hBMSC cultured in the absence of osteogenic supplements (OS+) under Single, Repeated, or Continuous exposure to 1, 5, or 10 µg/mL of 10 nm PVP-coated AgNP. Mineralization of the substrate is a late marker of osteogenic differentiation. Values plotted were derived by subtracting the signal values from OS- cells from the signals from OS+ supplemented cells. Therefore, the values plotted represent $\bar{x} \pm SD$ calculated as $\bar{X}_{OS+} - \bar{X}_{OS-} \pm \sqrt{SD_{OS+}^2 + SD_{OS-}^2}$ for n = 3 replicate experiments. Bars with asterisks denote a significant (p < 0.05) increase in mineralization of the substrate from OS+ supplemented cells over the corresponding OS- cells. Absent bars marked with ‡ are the result of negative values due to subtracting signal values from OS- cells from near-baseline signal values from OS+ supplemented cells.

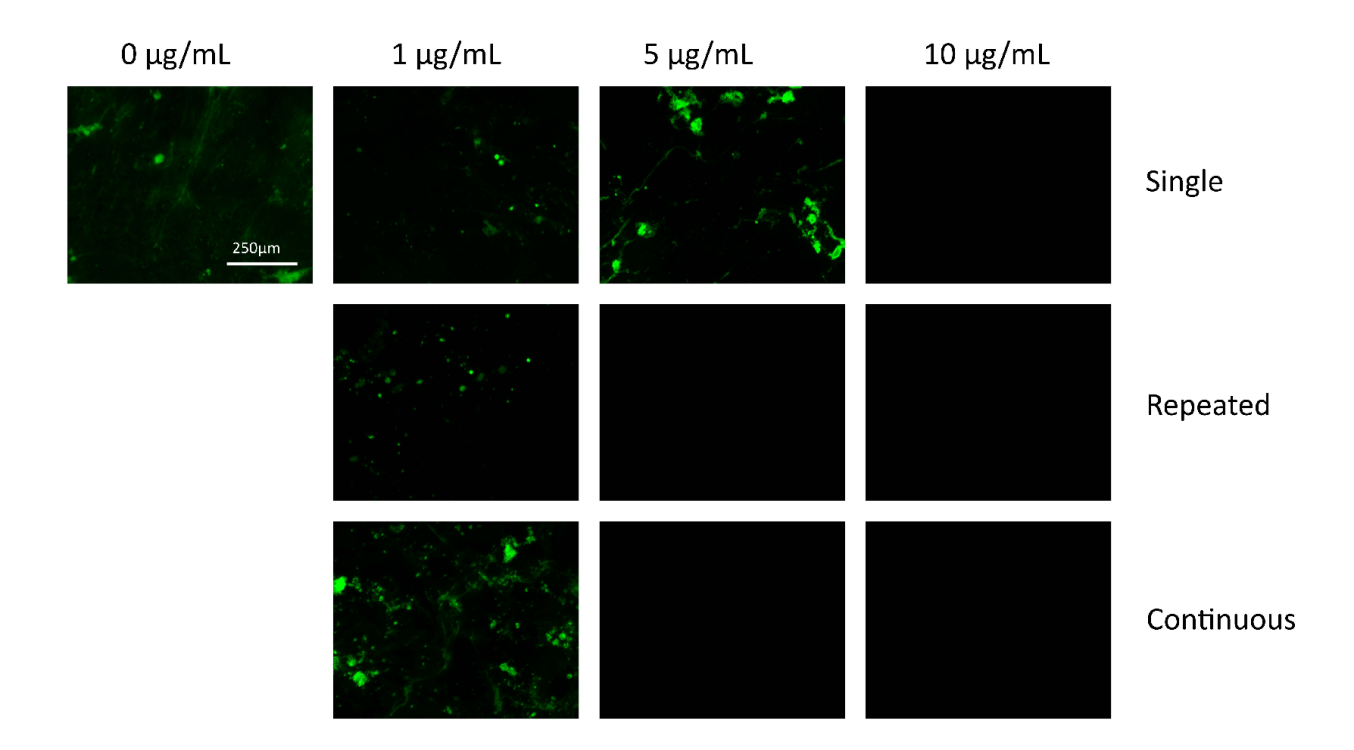


Figure 6 – Fluorescence microscopy images corresponding to the Osteoimage mineralization data summarized in Figure 7 for OS+ supplemented hBMSC cultured for 21 days and exposed to AgNP under Single, Repeated, or Continuous exposure scenarios. No hydroxyapatite was detected with Repeated or Continuous exposure to 5 μ g/mL AgNP or for any exposure to 10 μ g/mL AgNP.